ADVANCED FUNCTIONAL MATERIALS

DOI: 10.1002/adfm.200800320

Controllable Synthesis of Vertically Aligned p-Type GaN Nanorod Arrays on n-Type Si Substrates for Heterojunction Diodes**

By *Yong-Bing Tang, Xiang-Hui Bo, Chun-Sing Lee,* Hong-Tao Cong,* Hui-Ming Cheng, Zhen-Hua Chen, Wen-Jun Zhang, Igor Bello,* and *Shuit-Tong Lee**

A new catalyst seeding method is presented, in which aerosolized catalyst nanoparticles are continuously self-assembled onto amine-terminated silicon substrates in gas phase to realize controllable synthesis of vertically aligned Mg-doped GaN nanorod arrays on n-type Si (111) substrates. The diameter, areal density, and length of GaN nanorods can be controlled by adjusting the size of Au nanoparticles, flowing time of Au nanoparticles, and growth time, respectively. Based on the synthesis of p-type GaN nanorods on n-type Si substrates, p-GaN nanorod/n-Si heterojunction diodes are fabricated, which exhibit well-defined rectifying behavior with a low turn-on voltage of ~1.0 V and a low leakage current even at a reverse bias up to 10 V. The controllable growth of GaN nanorod arrays and the realization of p-type GaN nanorod/n-type Si heterojunction diodes open up opportunities for low-cost and high-performance optoelectronic devices based on these nanostructured arrays.

1. Introduction

One-dimensional (1D) nanostructures have been the focus of intensive investigations because of their potential applications in nanotechnology.[1–4] However, actual realization of 1D nanostructures for future nanoscale devices depends to a large extent on overcoming the challenge of synthesizing 1D nanostructures in an orderly manner because it is difficult to organize randomly distributed 1D nanostructures into designed positions due to their extremely small size,[5,6] even when micromanipulation or photolithography techniques are utilized.[7] There are many advantages associated with well-aligned 1D nanomaterial arrays that make them attractive for both fundamental investigations and practical applications in optoelectronic devices. Firstly, 1D nanostructure arrays are orderly, which can reduce much of the complicated assembling procedures needed in device fabrication. For example, such arrays have been directly used as functional components, such as electrodes of solar cells,[8] light-emitting diodes (LEDs),[9] nanolasers,[10] nanogenerators,[11] field emitters,[12] and so on. Secondly, well-aligned nanostructures provide good opportunities for exploring and understanding fundamental concepts about the roles of orderliness and dimensionality in physical properties. Furthermore, 1D nanostructure arrays grown on certain substrates may allow three-dimensional integration for more complex homo- or hetero-structures, such as vertical p-n junction diodes[6,13] and field-effect transistor arrays.[14] Since the preparation of oriented carbon nanotubes,[15] there has been a dramatic increase in the volume of research into 1D nanostructure arrays for a variety of materials, such as ZnO[8a,9–11,16] and Si.[17] However, up till now, controllable synthesis of well-aligned 1D nanostructure array in a simple way is still a challenge.

As an important III–V semiconductor, gallium nitride (GaN) has been extensively used in optoelectronic devices such as LEDs and laser diodes (LDs) due to its unique properties including wide band-gap and high carrier mobility.[18] Unlike some other wide band-gap materials, GaN can be reproducibly prepared with n- or p-type doping for semiconductor devices.[19] Compared to their thin-film count-

[*] Prof. C.-S. Lee, Prof. S.-T. Lee, Dr. Y.-B. Tang, Z.-H. Chen, Prof. W.-J. Zhang, Prof. I. Bello
Center of Super-Diamond and Advanced Films (COSDAF)
City University of Hong Kong
Hong Kong SAR (PR China)
E-mail: apcslee@cityu.edu.hk; apannale@cityu.edu.hk
Prof. C.-S. Lee, Dr. Y.-B. Tang, Z.-H. Chen, Prof. I. Bello
Department of Physics and Materials Science
City University of Hong Kong
Hong Kong SAR (PR China)
Prof. H.-T. Cong, X.-H. Bo, Prof. H.-M. Cheng
Shenyang National Laboratory for Materials Science
Institute of Metal Research
Chinese Academy of Sciences
Shenyang 110016 (PR China)
E-mail: htcong@imr.ac.cn
Prof. S.-T. Lee, Prof. W.-J. Zhang
Department of Physics and Materials Science
City University of Hong Kong
Hong Kong SAR (PR China)
Prof. S.-T. Lee, Prof. W.-J. Zhang
Technical Institute of Physics and Chemistry
Chinese Academy of Sciences
Beijing (PR China)

[**] This work was supported by a NSFC/RGC Joint Research Scheme (No. N_CityU 125/05) of Research Grants Council of Hong Kong SAR, China, the US Army International Technology Center – Pacific, and the National 973 projects of the Major State Research Development Program of China (Grant No. 2006CB933000 and Grant No. 2007CB936000).

erparts, 1D GaN nanostructures enable the fabrication of heterostructures with larger lattice mismatches.[13,20,21] GaN nanowires,[22] nanorods,[13,23] and core/shell nanorods[24] have already been used as building blocks for assembling electronic and optoelectronic nanodevices such as p-n junction diodes,[13] nano-LEDs,[22a,23,24] and nano-LDs.[25] Recently, researchers tried many methods to produce well-aligned 1D GaN nanostructure arrays to accelerate the practical applications in nanodevices. For example, single-crystal 1D GaN nanotube and nanorod arrays have been synthesized by metal-organic chemical vapor deposition.[26] By using metal-organic hydride vapor phase epitaxy, Kim et al. synthesized GaN multi-quantum-well nanorod arrays for high-brightness LEDs.[20,27] GaN nanowire arrays have also been synthesized by molecular beam epitaxy.[21,28] Combining silicon dioxide templates and organometallic vapor-phase epitaxy, Deb et al. prepared vertically aligned GaN nanorods.[13,29] Although these methods can yield highly crystalline 1D GaN nanostructured materials, relatively complicated fabricating systems and harsh synthesis conditions are often required, thus limiting their wide applications. In addition, metal-organic vapor sources are employed in most of these methods,[26–29] such as trimethylgallium, which are not only expensive but also harmful to environment and health. Therefore, controllable synthesis of well-ordered 1D GaN nanostructure arrays on substrates by a simple and cost-effective route is highly demanded.

In this study, we describe a new catalyst seeding method, in which aerosolized catalyst nanoparticles are self-assembled onto amine-terminated silicon substrates continuously in gas phase to realize controllable synthesis of vertically aligned Mg-doped GaN nanorod arrays on n-type Si (111) substrate. The diameter, density and length of these arrays are defined by gold (Au) catalyst nanoparticles. This method eliminates the lithographic steps used to fabricate p-n heterojunctions. Based on the synthesis of p-type GaN nanorods on n-type Si substrate, we fabricated p-GaN nanorod/n-Si heterojunction diode, which exhibits well-defined rectifying behavior with a low turn-on voltage of ca. 1.0 V.

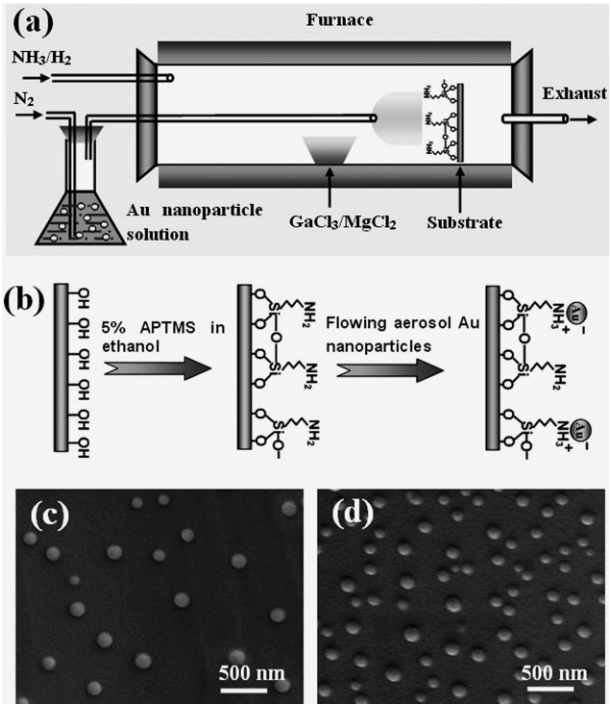

Figure 1. a) Schematic diagram of the apparatus for synthesizing the Mg-doped GaN nanorods by bubbling aerosolized Au nanoparticles as catalyst. b) Experimental strategy for the electrostatic assembly of Au nanoparticles on a Si substrate pre-modified with a APTMS monolayer. c) and d) SEM images of the Si substrates modified by bubbling 20 and 30 min of aerosolized Au nanoparticles, respectively.

2. Results and Discussion

Negatively charged Au nanoparticles in aqueous suspension were prepared by the trisodium citrate reduction of hydrogen tetrachloroaurate ($HAuCl_4$).[30] The Au nanoparticles were then carried by bubbling nitrogen through the suspension. The gas containing aerosolized Au nanoparticles was blow onto an amine-functionalized n-type Si (111) substrate in a chemical vapor deposition (CVD) chamber as shown schematically

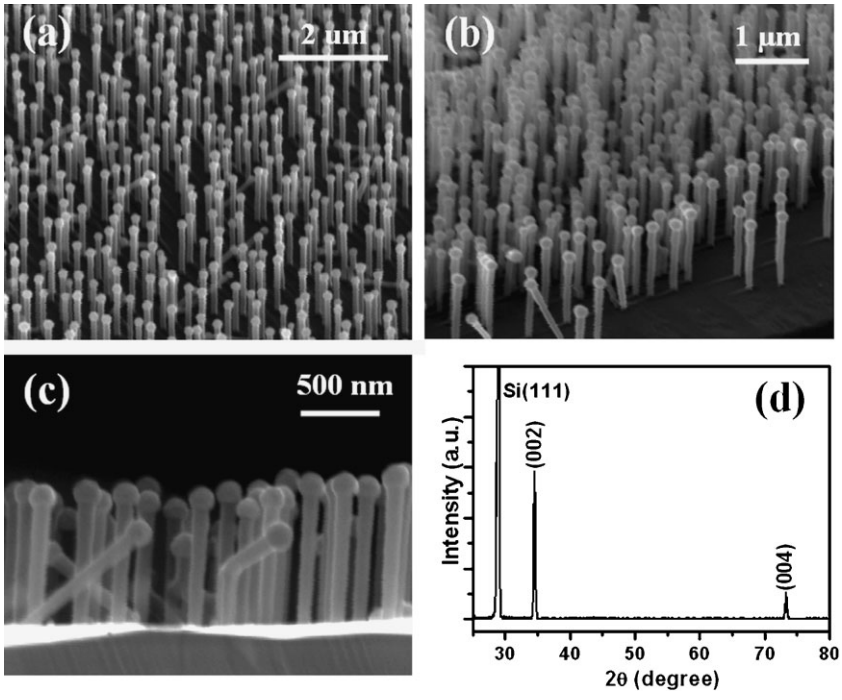

Figure 2. a–c) SEM images of Mg-doped GaN nanorod arrays. d) XRD spectrum of GaN nanorods on a Si substrate.

ADVANCED FUNCTIONAL MATERIALS

in Figure 1a. Encountering the aerosolized Au nanoparticles, the amine-functionalized Si substrate surface was partially protonated. Upon electrostatic interaction with the negatively charged nanoparticles,[31] an Au nanoparticle monolayer was formed (illustrated in Fig. 1b). The areal density of Au nanoparticles could be modified by changing the bubbling time. With increasing bubbling time, the areal density of Au nanoparticles on the substrate could be enhanced until a saturated monolayer was obtained. Figure 1c and d are scanning electron microscopy (SEM) images of the Si substrates functionalized by bubbling with 20 and 30 min of aerosolized Au nanoparticles.

The Mg-doped GaN nanorods were grown on the nanoparticle-seeded substrates by chloride CVD method using $GaCl_3$, $MgCl_2$, and NH_3 as Ga, Mg, and N precursors, respectively. The detailed synthesis process is described in the experimental section. The induction of Au catalyst nanoparticles led to a preferential growth direction of GaN nanorods with their *c*-axis normal to the substrate surface. Figure 2a–c show typical SEM images of the Mg-doped GaN nanorods grown from Au nanoparticles, the average diameter of which is ca. 150 nm at ca. 750 ° for 60 min growth (where the synthesis temperature refers to the temperature of the substrate surface). The tilted top-view SEM image (Fig. 2a) reveals a high density of GaN nanorods aligning uniformly on the substrate. No GaN buffer layer is observed from the SEM image (Fig. 2b) taken from the edge of substrate, confirming the aligned GaN nanorods were epitaxially grown on the Si substrate. A cross-section SEM image (Fig. 2c) shows that most of the nanorods are vertically oriented with respect to the Si (111) substrate surface, while a small fraction are in different orientations. The preferred orientation of the nanorods suggests that the epitaxial growth of 1D GaN nanostructures on a Si substrate is possible. The diameters of the nanorods are in the range of 60–120 nm with an average value of 90 nm, and the lengths are 0.8–1.2 μm. The areal density of the nanorod array is ca. $2.0 \times 10^9\,cm^{-2}$. Figure 2d presents the X-ray diffraction (XRD) spectrum of the aligned GaN nanorod arrays on the Si(111) substrate. Only diffraction peaks from (002) and (004) crystal planes of wurtzite GaN are observed, indicating a good alignment of nanorods and the epitaxial relationship of GaN(001)//Si(111) between the nanorods and the Si substrate in despite of their large lattice mismatch. No characteristic peaks associated with Au phase were detected in the XRD pattern, revealing that the Au content was below the detection limit of XRD.

Transmission electron microscopy (TEM) characterizations confirm that the nanorods are single-crystalline GaN with [001] growth direction. Figure 3a is a typical bright-field TEM image of an individual GaN nanorod. The strong contrast between the nanorod and Au catalyst nanoparticle indicates a clear interface between the two crystal phases. Energy-dispersive X-ray spectroscopy (EDS) analyses reveal that the nanorod is composed of Ga, N, and Mg elements with an atomic ratio of ca. 48.1:50.4:1.5. Composition distribution was determined by the EDS elemental mapping (Fig. 3b–d). It can be seen that the

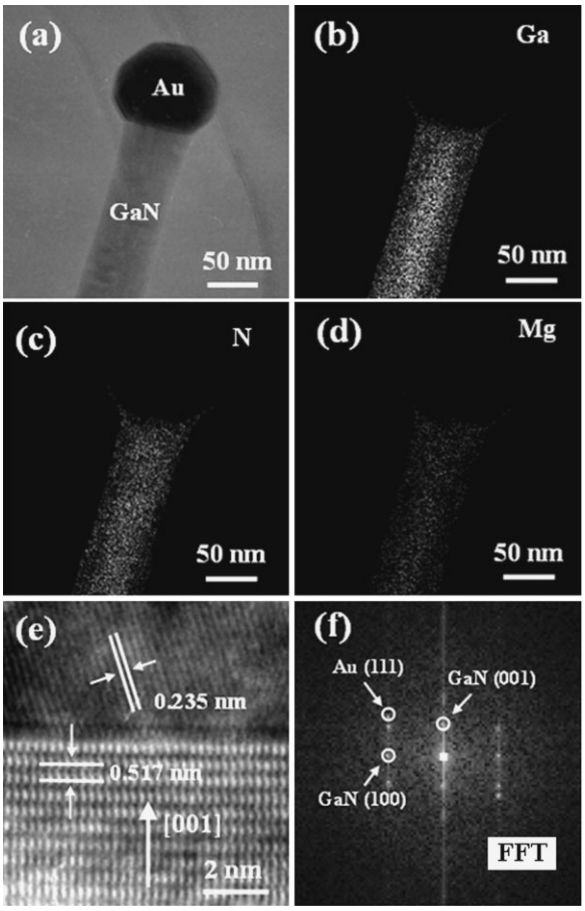

Figure 3. TEM image of a typical GaN nanorod (a), and its corresponding Ga (b), N (c), and Mg (d) EDS elemental mappings. e) HRTEM image of the interface of GaN nanorod and Au catalyst nanoparticle. f) Fast Fourier transformation (FFT) pattern of the HRTEM image.

Mg element is uniformly distributed in the GaN nanorod. EDS analyses on various nanorods show that the content of Mg varies from 1.1 to 2.4 at%. Figure 3e presents the HRTEM image taken from the interface between the catalyst tip and the nanorod. Along the nanorod the adjacent lattice distance is ca. 0.52 nm, which is close to the *d*-spacing of (001) crystal plane (0.517 nm) of wurtzite GaN, and further confirms the (001) crystallographic growth direction of the nanorods. On the catalyst side, the crystal lattices with a spacing of ca. 0.235 nm correspond to the (111) plane of body-centered Au. The crystallographic relationship between the GaN nanorods and Au revealed by the corresponding fast Fourier transformation pattern (Fig. 3f) is GaN(001)//Au(111). Both of the TEM and EDS analyses verify that the GaN nanorods are single-crystalline in nature and doped with Mg element, and TEM investigations on other nanorods also give similar results.

The presence of gold nanoparticle at the tip of each GaN nanorods suggests that the catalyst-induced vapor-liquid-solid (VLS) mechanism controls the whole growth process. Since each Au nanoparticle seeds the growth of one nanorod, this approach will be very useful for precise pattern fabrication. The nanorods tend to taper from top to bottom, with diameters

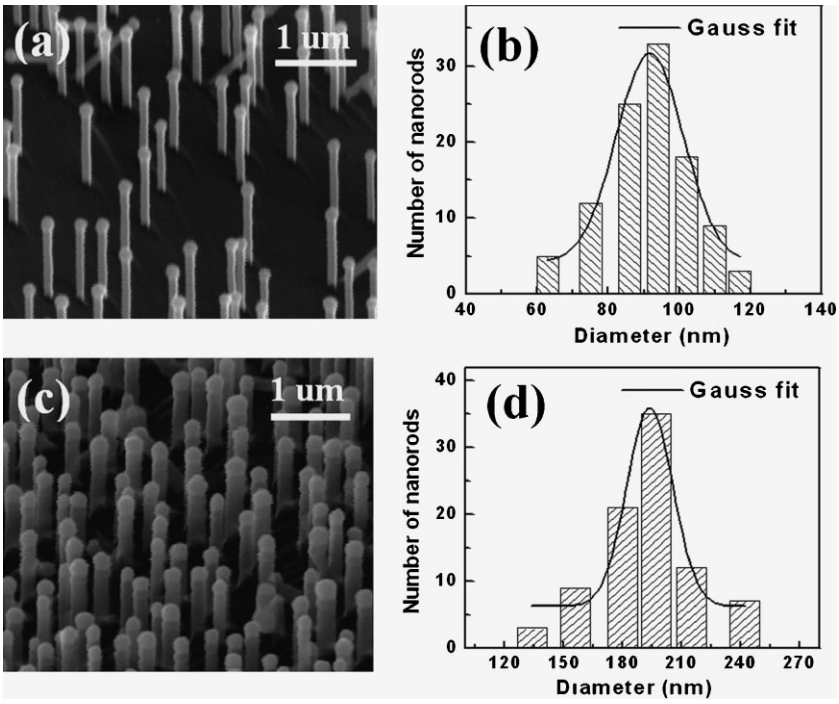

Figure 4. a,c) SEM image of the GaN nanorods grown from Au nanoparticles with diameters of (153 ± 35) and (236 ± 78) nm, respectively. b) and d) Size distributions of the nanorods with average diameters of ca. 92 and ca. 187 nm, respectively.

smaller than those of Au nanoparticles. The reason for this phenomenon can be explained as follows: The growth rate of the GaN nanorods in the axial direction far exceeds that in the radial direction, resulting in a rod-like morphology. On increase of the growth time, the nanorods started growing laterally and the uncatalyzed growth on the sidewalls of nanorods leads to a taper morphology similar to previous reports.[21a,29a] Although the nanorod diameters are smaller than their respective seed particles, they have approximately the same relative standard deviation of diameters as that of Au nanoparticles. Figure 4a and c show that the GaN nanorod arrays grown from Au nanoparticles with diameters of (153 ± 35) and (236 ± 78) nm are ~92 and ~187 nm in average diameter, respectively. The standard deviations (Fig. 4b and d) of the diameters of the nanorods grown from Au nanoparticles are 19.7% and 39.3%, respectively. Therefore, by seeding Au catalyst nanoparticles with a specific size, we are able to control the average diameter of the GaN nanorods.

Through adjusting the flowing time of aerosolized Au nanoparticles onto the amine-functionalized Si substrate, controllable density of well-aligned GaN nanorod arrays can be achieved. With increasing flowing time, the areal density of Au particles on the substrate can be enhanced until a saturated Au nanoparticle monolayer was obtained. Figure 5a and b are SEM images of two samples under similar experimental conditions except for the different flowing time of aerosolized Au nanoparticles. There was a marked difference in the areal density of the two nanorod arrays. For 10 min flowing time, the nanorod density was low and of the order of $(0.9 \pm 0.6) \times 10^8$ nanorods cm^{-2} (Fig. 5a), while for 30 min flowing time, the density already increased to above $(9.2 \pm 1.5) \times 10^8$ nanorods cm^{-2} (Fig. 5b). The areal density of nanorod arrays increased from ca. 1.0 to ca. $20.0 \times 10^8\,cm^{-2}$ as the flowing time increased from 10 min to 70 min (Fig. 5c). However, when the flowing time reached 60 min, the nanorod density became saturated, from which we assume the electrostatic interaction between the catalyst nanoparticles and free amine-terminated substrate to be completed. At the initial stage of the flow of Au nanoparticles, the density of catalyst nanoparticles increases gradually. For longer flowing time, the density becomes saturated due to the decrease of free amine functional groups as a result of continuous adsorption of the Au nanoparticles. The density control of nanorod arrays is very important for some applications such as field emission because an optimal density is needed for aligned nanostructures to avoid the field screening effect.[32]

Length of the GaN nanorods can be controlled by adjusting the growth duration. Figure 6a and b are the SEM images of the samples grown for 20 and 50 min, respectively. Although the diameter of nanorods also changes slightly with increasing growth time, the change in length is much more obvious. On increasing growth time, the length of nanorods increased dramatically. Figure 6c reveals that there is a rapid increase of the nanorod length with growth time between 10 and 40 min. After 20 min growth, the length is about 350 nm (Fig. 6a), while for 50 min growth, the length is above 950 nm, which is almost the maximum observed length (Fig. 6b). The initial length increase of the nanorods resulted from the continuous precipitation of solid GaN from the supersaturated alloy droplets. However, the growth rate of GaN nanorods decreased with increasing length due to the decrease in temperature away from the substrate surface, thus resulting in nanorod length saturation.

Electron transport measurements on GaN nanorod arrays were carried out by fabricating a p-n diode structure directly on the as-prepared p-GaN nanorod/n-Si substrate sample. A thin insulating photoresist was deposited in the inter space of a GaN nanorod array (ca. 10×10^8 nanorods cm^{-2}) by spin coating for separating individual nanorods. Note that it was not possible to fabricate functional diode structures from the nanorod arrays with densities higher than 15×10^8 nanorod cm^{-2} for the difficulty in depositing of photoresist into the narrow intervals between nanorods. After deposition of photoresist, the surface of the sample was partially dissolved by acetone until the tips of GaN nanorods were exposed for metal contact. Figure 7a is an atomic force microscopy (AFM) image of the structure showing the exposed GaN nanorod tips. Ohmic metal contacts

ADVANCED FUNCTIONAL MATERIALS

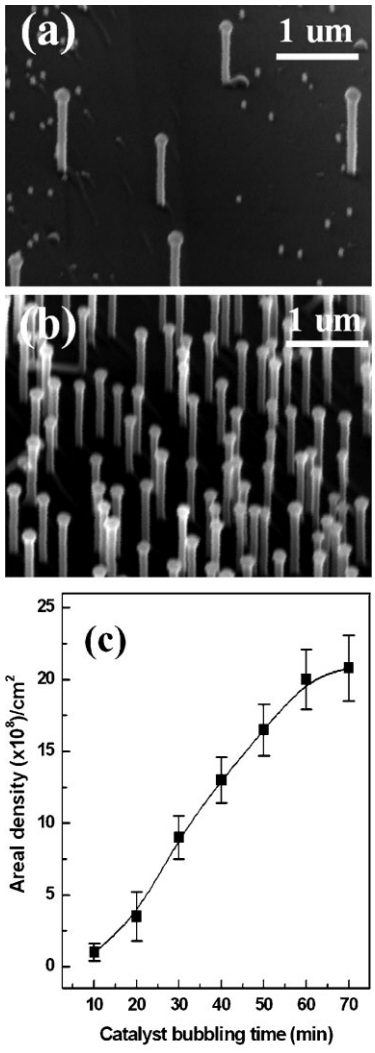

Figure 5. a,b) SEM images of two nanorod samples grown on the Si substrates modified with 10 and 30 min of aerosolized Au nanoparticles flowing times. c) Areal density of GaN nanorods as a function of the bubbling time of the aerosolized Au nanoparticles.

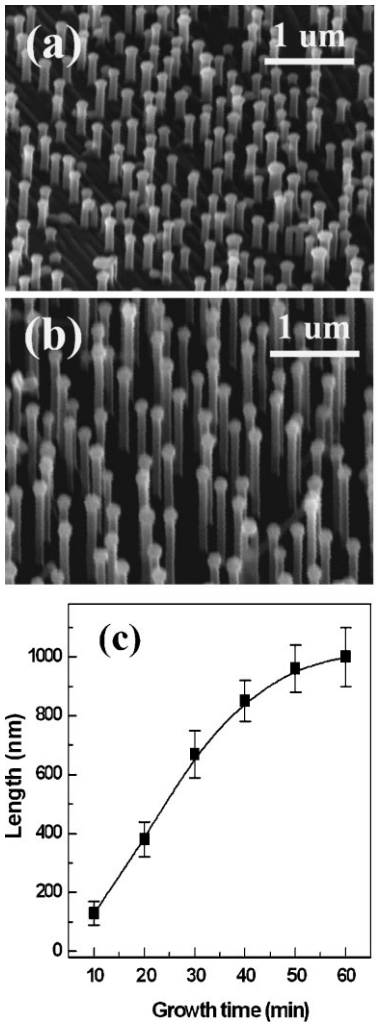

Figure 6. SEM images of two nanorod samples grown for 20 (a) and 50 min (b). c) GaN nanorod length plotted as a function of the growth time.

were obtained by electron-beam evaporating Ni/Au and Ti/Al electrodes on p-type GaN nanorods and n-type Si substrate, respectively. The final schematic structure of the p-n heterojunction diode is shown in Figure 7b.

The current–voltage (I–V) characteristic curve of the fabricated heterojunction diode at room temperature is shown in Figure 8a, exhibiting a well-defined rectifying behavior with a low turn-on voltage of about 1.0 V in forward bias. The reverse leakage current is less than 0.3 mA at a reverse bias up to 10 V. The I-V characteristics of practical diodes are described by the simplified diode equation:[33]

$$I = I_0[\exp(eV/\eta kT) - 1]$$

where I is the forward current, I_0 is the reverse saturation current, e is the electronic charge, V is the forward-bias voltage, k is the Boltzmann's constant, T is absolute temperature, and η is the ideality factor. For forward voltages larger than the thermal voltage kT/e, the corresponding $\log(I)$ versus V plot (inset, Fig. 8a) has an approximate linear segment and the ideality factor η obtained from the slope of the linear segment of the above plot is 3.4 ± 0.7. This ideality factor is consistent with those of previously reported GaN nanorod (11.2 ± 0.56)[13] and nanowire (5.5–6.5)[34] p-n junction diodes, and also consistent with the results reported for standard thin-film GaN p-n diodes (2.5–6.9).[35] However, the high ideality factor (>2) of GaN-based p-n junction diodes is not fully understood.[35] Such high values are commonly attributed to carrier tunneling via deep levels in the space charge region due to high doping concentration or high-density localized states.[35a–c]

The transport mechanism and low turn-on voltage of the p-GaN nanorod/n-Si heterojunction diode can be understood from the energy band structure of the heterostructure. Figure 8b shows the schematic energy band diagrams of the heterojunction diode at thermal equilibrium (left) and under forward bias (right). It is well known that the barrier height

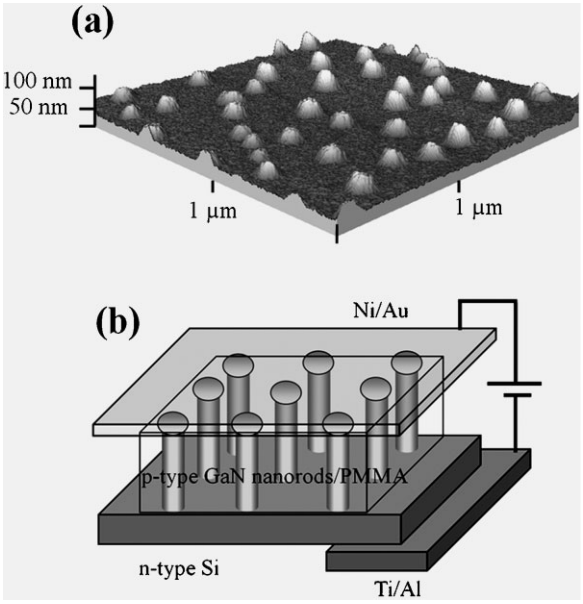

Figure 7. a) Three-dimensional AFM image of GaN nanorod tips exposed above the PMMA layer. b) A schematic of the p-GaN nanorod/n-Si heterojunction diodes for *I–V* measurement.

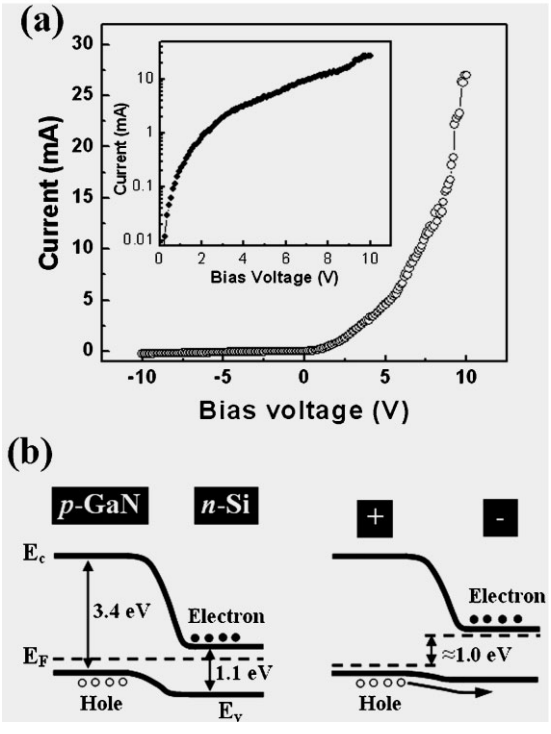

Figure 8. a) The *I–V* characteristics of the p-GaN nanorods/n-Si heterojunction illustrating well-defined rectifying behavior. The inset shows the forward bias *I–V* characteristics on a logarithmic scale. b) Schematic energy band diagrams of the p-GaN nanorods/n-Si heterojunction diode at thermal equilibrium (left) and under forward bias (right).

decreases when a forward bias is applied to a p-n junction. In the present case, the band gap energy is quite different between p-type GaN (3.4 eV) and n-type Si (1.1 eV), so the barrier region is not symmetrical. When a negative voltage is applied to the n-type Si, the heterojunction is under forward bias and the valence band maximum (E_V) of Si moves to a higher energy level. When the forward bias is increased, E_V(Si) approaches the E_v of p-GaN and the barrier to the hole carriers disappears under a forward bias of about 1.0 V. Then the hole can transport readily from the E_v(GaN) to the E_v (Si), giving rise to the conduction current. Therefore, the p-n heterojunction can be turned on by a low threshold voltage of about 1.0 V. This p-n heterojunction behavior is highly reproducible and remains unchanged in a period of eight months.

3. Conclusion

We have presented a simple and controllable route to produce vertically aligned Mg-doped GaN nanorod arrays on n-type Si substrate by flowing aerosolized Au nanoparticles as catalysts in a conventional CVD furnace. The diameter, areal density and length of GaN nanorods can be controlled by adjusting the size of Au nanoparticles, flowing time of Au nanoparticles, and the growth time, respectively. We expect that this method can also be readily generalized to synthesize other types of well-aligned 1D nanostructures on various substrates. With the p-type GaN nanorod arrays on n-type Si, we have fabricated p-GaN nanorod/n-Si heterojunction diodes. Transport measurements revealed that this heterojunction exhibited well-defined and reliable rectifying behavior. The p-n heterojunction diodes showed a low turn-on voltage of ca. 1.0 V and a low leakage current even at a reverse bias up to 10 V. The controllable growth of GaN nanorod arrays and the realization of p-type GaN nanorod/n-type Si heterojunction diode open up opportunities for low-cost and high-performance optoelectronic devices based on these nanostructure arrays.

4. Experimental

Negatively charged gold nanoparticles in aqueous suspension were prepared by reducting of hydrogen tetrachloroaurate ($HAuCl_4$) with trisodium citrate [30], and the diameters of the nanoparticles were controlled by changing the molar ratio of $HAuCl_4$ to trisodium citrate [36]. N-type Si (111) substrates ($1 \times 2\,cm^2$) were cleaned by immersion in a piranha solution (3:1 H_2SO_4:30% H_2O_2) at 80 °C for 10 min and washed with deionized water in order to get the maximum number of exposed surface –OH groups. The substrates were then immersed into a 5% solution of 3-aminopropyltrimethoxysilane (APTMS, Aldrich) in ethanol for 20 min, then rinsed three times with deionized water, and dried at 90 °C for 10 min. Finally, the modified Si substrate was vertically placed on the downstream of a horizontal CVD furnace, and the Au nanoparticle solutions were directly pumped to the substrate by bubbling nitrogen (150 sccm) through a vessel containing Au nanoparticles in liquid state, as shown schematically in Figure 1a. The surface of the modified substrate was partially protonated. Upon

ADVANCED FUNCTIONAL MATERIALS

interaction with the negatively charged Au nanoparticles, the electrostatically driven assembly of an Au nanoparticle layer took place. Aerosolized catalyst nanoparticles were self-assembled onto the amine-terminated Si substrates continuously in gas phase, therefore, the bubbling time can influence the areal density of Au nanoparticles. With increasing bubbling time, the areal density of Au nanoparticles on the substrate could be increased until a saturated monolayer was obtained. Before use, the Au nanoparticle-seeded Si substrates were annealed at 500 °C in a hydrogen atmosphere for 20 min to remove the organic groups.

The Mg-doped GaN nanorods were grown by a simple CVD method. A mixture of $GaCl_3$ powder and $MgCl_2$ powder with a molar ratio of 30:1 was used as the starting source. The premixed source powder was loaded into an alumina boat and positioned at the center of an alumina tube that was inserted into a horizontal CVD furnace. The Au nanoparticle-seeded Si substrate was placed at a fixed distance (5–10 cm, downstream) from the alumina boat. NH_3 with 5% H_2 was employed as the reactant gases and flowed continuously in the direction from the source powder to the substrate at a rate of 100 sccm. The source was heated up from room temperature at a ramping rate of 30 °C min^{-1} to and maintained at about 850 °C. Correspondingly, the substrate temperature was kept at about 700–750 °C for the nanorods growth. Typical growth time lasted from 10 to 60 minutes, and the reactions were carried out at atmospheric pressure.

The as-synthesized GaN nanorod arrays were light yellow in color. The morphology, phase purity, structural characterization, and elemental composition analysis of the GaN nanorods were investigated by using field-emission scanning electron microscopy (SEM, Philips XL30 FEG), X-ray diffraction (XRD, Rigaku D/max-2400) and high-resolution transmission electron microscopy (HRTEM, Tecnai F30) equipped with an energy dispersive X-ray spectroscopy (EDS, Oxford INCA).

Electron transport measurements of GaN nanorod arrays were carried out by fabricating p-n junction diode structure directly on the p-GaN nanorod/n-Si substrate sample. Before fabrication, the oxide formed on the n-Si substrate was etched away with 2% HF. A thin insulating photoresist (PMMA) was spin-coated to fill the interspace of a GaN nanorod array with a density of ca. 10×10^8 nanorods cm^{-2}. The surface of the PMMA layer was then partially dissolved by acetone to expose the tips of the GaN nanorods for fabricating metal contacts. Ohmic contacts were achieved by electron-beam evaporating Ni/Au (30/50 nm) and Ti/Al (30/50 nm) electrodes onto the p-type GaN nanorods and the backside of n-type Si substrate, respectively. The current–voltage (I–V) properties of the devices were measured by applying a DC voltage to the device using a source meter (Keithley 487).

Received: March 6, 2008
Revised: June 10, 2008

[1] a) C. M. Lieber, *MRS Bull.* **2003**, *28*, 486. b) Y. Li, F. Qian, J. Xiang, C. M. Lieber, *Mater. Today* **2006**, *9*, 18. c) C. M. Lieber, Z. L. Wang, *MRS Bull.* **2007**, *32*, 99.

[2] a) P. Yang, *MRS Bull.* **2005**, *30*, 85. b) P. J. Pauzauskie, P. Yang, *Mater. Today* **2006**, *9*, 36.

[3] Y. Xia, P. Yang, Y. Sun, Y. Wu, B. Mayers, B. Gates, Y. Yin, F. Kim, H. Yan, *Adv. Mater.* **2003**, *15*, 353.

[4] Z. L. Wang, *Mater. Today* **2004**, *7*, 26.

[5] a) M. Huang, S. Mao, H. Feick, H. Yan, Y. Wu, H. Kind, E. Weber, R. Russo, P. Yang, *Science* **2001**, *292*, 1897. b) X. D. Wang, C. J. Summers, Z. L. Wang, *Nano Lett.* **2004**, *4*, 423. c) X. D. Wang, J. Song, P. Li, J. H. Ryou, R. D. Dupuis, C. J. Summers, Z. L. Wang, *J. Am. Chem. Soc.* **2005**, *127*, 7920.

[6] J. J. Wu, D. K. P. Wong, *Adv. Mater.* **2007**, *19*, 2015.

[7] a) J. S. Jie, W. J. Zhang, Y. Jiang, X. M. Meng, Y. Q. Li, S. T. Lee, *Nano Lett.* **2006**, *6*, 1887. b) J. S. Jie, W. J. Zhang, Y. Jiang, S. T. Lee, *Appl. Phys. Lett.* **2006**, *89*, 133118.

[8] a) M. Law, L. E. Greene, J. C. Johnson, R. Saykally, P. Yang, *Nat. Mater.* **2005**, *4*, 455. b) G. K. Mor, K. Shankar, M. Paulose, *Nano Lett.* **2006**, *6*, 215. c) K. Peng, Y. Xu, Y. Wu, Y. Yan, S. T. Lee, J. Zhu, *Small* **2005**, *1*, 1062.

[9] W. I. Park, G. C. Yi, *Adv. Mater.* **2004**, *16*, 87.

[10] a) M. H. Huang, S. Mao, H. Feick, H. Yan, Y. Wu, H. Kind, E. Weber, R. Russo, P. Yang, *Science* **2001**, *292*, 1897. b) J. H. Choy, E. S. Jang, J. H. Won, J. H. Chung, D. J. Jang, Y. W. Kim, *Adv. Mater.* **2003**, *15*, 1911.

[11] a) Z. L. Wang, J. Song, *Science* **2006**, *312*, 242. b) P. G. Gao, J. H. Song, J. Liu, Z. L. Wang, *Adv. Mater.* **2007**, *19*, 67. c) Z. L. Wang, *MRS Bull.* **2007**, *32*, 109. d) Z. L. Wang, *Adv. Mater.* **2007**, *19*, 889. d) X. D. Wang, J. H. Song, J. Liu, Z. L. Wang, *Science* **2007**, *316*, 102.

[12] a) Y. W. Zhu, H. Z. Zhang, X. C. Sun, S. Q. Feng, J. Xu, Q. Zhao, B. Xiang, R. M. Wang, D. P. Yu, *Appl. Phys. Lett.* **2003**, *83*, 144. b) J. H. He, R. Yang, Y. L. Chueh, L. J. Chou, L. J. Chen, Z. L. Wang, *Adv. Mater.* **2006**, *18*, 650. c) Y. B. Tang, H. T. Cong, Z. G. Zhao, H. M. Cheng, *Appl. Phys. Lett.* **2005**, *86*, 153104. d) Y. B. Tang, H. T. Cong, Z. M. Wang, H. M. Cheng, *Appl. Phys. Lett.* **2005**, *89*, 253112.

[13] P. Deb, H. Kim, Y. Qin, R. Lahiji, M. Oliver, R. Reifenberger, T. Sands, *Nano Lett.* **2006**, *6*, 2893.

[14] a) W. B. Choi, J. U. Chu, K. S. Jeong, E. J. Bae, J. W. Lee, J. J. Kim, J. O. Lee, *Appl. Phys. Lett.* **2001**, *79*, 3696. b) H. Ng, J. Han, T. Yamada, P. Nguyen, Y. P. Chen, M. Meyyappan, *Nano Lett.* **2004**, *4*, 1247.

[15] a) W. Z. Li, S. S. Xie, L. X. Qian, B. H. Chang, B. S. Zou, W. Y. Zhou, R. A. Zhao, G. Wang, *Science* **1996**, *274*, 1701. b) Z. F. Ren, Z. P. Huang, J. W. Xu, J. H. Wang, P. Bush, M. P. Siegal, P. N. Provencio, *Science* **1998**, *282*, 1105.

[16] a) X. D. Wang, J. Zhou, C. S. Lao, J. H. Song, N. S. Xu, Z. L. Wang, *Adv. Mater.* **2007**, *19*, 1627. b) S. H. Jung, E. Oh, K. H. Lee, W. Park, S. H. Jeong, *Adv. Mater.* **2007**, *19*, 749. c) G. D. Yuan, W. J. Zhang, J. S. Jie, X. Fan, J. X. Tang, I. Shafiq, Z. Z. Ye, C. S. Lee, S. T. Lee, *Adv. Mater.* **2008**, *20*, 168.

[17] a) K. Q. Peng, Y. J. Yan, S. P. Gao, J. Zhu, *Adv. Mater.* **2002**, *14*, 1164. b) K. Peng, M. Zhang, A. Lu, N. B. Wong, R. Zhang, S. T. Lee, *Appl. Phys. Lett.* **2007**, *90*, 163123. c) A. I. Hochbaum, R. Fan, R. He, P. Yang, *Nano Lett.* **2005**, *5*, 457.

[18] a) S. Nakamura, T. Mukai, M. Senoh, *J. Appl. Phys.* **1994**, *76*, 8189. b) S. Nakamura, *Adv. Mater.* **1996**, *8*, 689. c) H. Morkoc, S. N. Mohammand, *Science* **1996**, *267*, 51. d) F. A. Ponce, D. P. Bour, *Nature* **1997**, *386*, 251.

[19] a) S. Nakamura, *Science* **1998**, *281*, 956. b) S. Nakamura, M. Senoh, N. Iwasa, S. Nagahama, T. Yamada, T. Mukai, *Jpn. J. Appl. Phys. Part 2* **1995**, *34*, L1332.

[20] H. M. Kim, Y. H. Cho, H. Lee, S. I. Kim, S. R. Ryu, D. Y. Kim, T. W. Kang, K. S. Chung, *Nano Lett.* **2004**, *4*, 1059.

[21] a) R. Calarco, R. J. Meijers, R. K. Debnath, T. Stoica, E. Sutter, H. Luth, *Nano Lett.* **2007**, *7*, 2248. b) R. Meijers, T. Richter, R. Calarco, T. Stoica, H. P. Bochem, M. Marso, H. Luth, *J. Cryst. Growth* **2006**, *289*, 381. c) N. Thillosen, K. Sebald, H. Hardtdegen, R. Meijers, R. Calarco, S. Montanari, N. Kaluza, J. Gutowski, H. Luth, *Nano Lett.* **2006**, *6*, 704.

[22] a) Z. H. Zhong, F. Qian, D. Wang, C. M. Lieber, *Nano Lett.* **2003**, *3*, 343. b) Y. Huang, X. Duan, Y. Cui, C. M. Lieber, *Nano Lett.* **2002**, *2*, 101. c) H. J. Choi, H. K. Seong, J. Chang, K. I. Lee, Y. J. Park, J. J. Kim, S. K. Lee, R. He, T. Kuykendall, P. Yang, *Adv. Mater.* **2005**, *17*, 1351. d) J. R. Kim, H. Oh, H. M. So, J. J. Kim, J. Kim, C. J. Lee, S. C. Lyu, *Nanotechnology* **2002**, *13*, 701.

[23] a) H. M. Kim, D. S. Kim, Y. S. Park, D. Y. Kim, T. W. Kang, K. S. Chung, *Adv. Mater.* **2003**, *15*, 991.

[24] a) F. Qian, Y. Li, S. Gradecak, D. L. Wang, C. J. Barrelet, C. M. Lieber, *Nano Lett.* **2004**, *4*, 1975. b) F. Qian, S. Gradecak, Y. Li, C. Y. Wen, C. M. Lieber, *Nano Lett.* **2005**, *5*, 2287.

[25] a) J. C. Johnson, H. J. Choi, K. P. Knutsen, R. D. Schaller, P. D. Yang, R. J. Saykally, *Nat. Mater.* **2002**, *1*, 106. b) P. J. Pauzauskie, D. J. Sirbuly, P. D. Yang, *Phys. Rev. Lett.* **2006**, *96*, 143903.

[26] a) J. Goldberger, R. R. He, Y. F. Zhang, S. W. Lee, H. Q. Yan, H. J. Choi, P. D. Yang, *Nature* **2003**, *422*, 599. b) T. Kuykendall, P. J. Pauzauskie, Y. F. Zhang, J. Goldberger, D. Sirbuly, J. Denlinger, P. D. Yang, *Nat. Mater.* **2004**, *3*, 524. c) H. D. Hersee, X. Sun, X. Wang, *Nano Lett.* **2006**, *6*, 1808. d) X. Wang, X. Y. Sun, M. Fairchild, S. D. Hersee, *Appl. Phys. Lett.* **2006**, *89*, 233115. e) G. Kipshidze, B. Yavich, A. Chandolu, J. Yun, V. Kuryatkov, I. Ahmad, D. Aurongzeb, M. Holtz, H. Temkin, *Appl. Phys. Lett.* **2005**, *86*, 033104.

[27] Y. P. Sun, Y. H. Cho, H. M. Kim, T. W. Kang, *Appl. Phys. Lett.* **2005**, *87*, 093115.

[28] a) L. W. Tu, C. L. Hsiao, T. W. Chi, I. Lo, K. Y. Hsieh, *Appl. Phys. Lett.* **2003**, *82*, 1601. b) Y. S. Park, C. M. Park, D. J. Fu, T. W. Kang, J. E. Oh, *Appl. Phys. Lett.* **2004**, *85*, 5718. c) H. Y. Chen, H. W. Lin, C. H. Shen, S. Gwo, *Appl. Phys. Lett.* **2006**, *89*, 243105.

[29] a) P. Deb, H. Kim, V. Rawat, M. Oliver, S. Kim, M. Marshall, E. Stach, T. Sands, *Nano Lett.* **2005**, *5*, 1847. b) J. Yoo, Y. J. Hong, S. J. An, G. C. Yi, B. Chon, T. Joo, J. W. Kim, J. S. Lee, *Appl. Phys. Lett.* **2006**, *89*, 043124.

[30] G. Frens, *Nature Phys. Sci.* **1973**, *211*, 20.

[31] a) N. A. Kotov, I. Dekany, J. H. Fendler, *J. Phys. Chem.* **1995**, *99*, 13065. b) D. L. Feldheim, K. C. Grabar, M. J. Natan, T. E. Mallouk, *J. Am. Chem. Soc.* **1996**, *118*, 7640. c) J. Schmitt, G. Decher, W. J. Dressick, S. L. Brandow, R. E. Geer, R. Shashidhar, J. M. Calvert, *Adv. Mater.* **1997**, *9*, 61. d) A. N. Shipway, M. Lahav, I. Willner, *Adv. Mater.* **2000**, *12*, 993.

[32] a) S. H. Jo, J. Y. Lao, Z. F. Ren, R. A. Farrer, T. Baldacchini, J. T. Fourkas, *Appl. Phys. Lett.* **2003**, *83*, 4821. b) S.-H. Jeong, H.-Y. Hwang, K.-H. Lee, Y. Jeong, *Appl. Phys. Lett.* **2001**, *78*, 2052.

[33] D. A. Neamen, *Semiconductor Physics and Devices: Basic Principles*, McGraw-Hill, New York **2003**, p. 304.

[34] G. Cheng, A. Kolmakov, Y. Zhang, M. Moskovits, R. Munden, A. M. Reed, G. Wang, D. Moses, *Appl. Phys. Lett.* **2003**, *83*, 1578.

[35] a) H. C. Casey, J. Muth, S. Krishnankutty, J. M. Zavada, *Appl. Phys. Lett.* **1996**, *68*, 2867. b) P. Perlin, M. Osinsky, P. G. Eliseev, V. A. Smagley, J. Mu, M. Banas, P. Sartori, *Appl. Phys. Lett.* **1996**, *69*, 1680. c) V. A. Dmitriev, *MRS Internet J. Nitride Semicond. Res.* **1996**, *1*, 29. d) J. M. Shah, Y. L. Li, T. Gessmann, E. F. Schubert, *Appl. Phys. Lett.* **2003**, *94*, 2627. e) A. Chitnis, A. Kumar, M. Shatalov, V. Adivarahan, A. Lunev, J. W. Yang, G. Simin, M. Asif Khan, R. Gaska, M. Shur, *Appl. Phys. Lett.* **2000**, *77*, 3800.

[36] a) A. Doron, E. Katz, I. Willner, *Langmuir* **1995**, *11*, 1313. b) A. N. Shipway, E. Katz, I. Willner, *Chem. Phys. Chem.* **2000**, *1*, 18.